Materials Research Bulletin 47 (2012) 3580–3585

Contents lists available at SciVerse ScienceDirect

Materials Research Bulletin

journal homepage: www.elsevier.com/locate/matresbu

Phase equilibria in the system $NaAl(WO_4)_2$–$NaCr(WO_4)_2$

I. Koseva *, A. Yordanova, D. Rabadjieva, P. Tzvetkov, V. Nikolov

Institute of General and Inorganic Chemistry, Bulgarian Academy of Sciences, Acad. G. Bonchev Str., Building 11, 1113 Sofia, Bulgaria

ARTICLE INFO

Article history:
Received 9 March 2012
Received in revised form 22 May 2012
Accepted 14 June 2012
Available online 29 June 2012

Keywords:
A. Optical materials
B. Chemical synthesis
C. Electron diffraction
C. X-ray diffraction

ABSTRACT

The phase equilibria in the system $NaAl(WO_4)_2$–$NaCr(WO_4)_2$ are investigated. Nanopowders are synthesized in the whole concentration region from $NaAl(WO_4)_2$ to $NaCr(WO_4)_2$ by a co-precipitation method. Using X-ray, DTA, TEM and SEM analyses, three concentration regions in the system are established: single-phase region of $NaAl_{1-x}Cr_x(WO_4)_2$ solid solutions (x is between 0 and 0.08), with monoclinic structure, space group C2/c; single-phase region of $NaAl_{1-x}Cr_x(WO_4)_2$ solid solutions (x is between 0.40 and 1.0) with monoclinic structure, space group P2/c; and two-phase region, where the above mentioned phases crystallize simultaneously (x is between 0.08 and 0.40). The thermal behaviour of the two pure boundary phases, as well as the influence of chromium on the thermal stability and the structural characteristics of the solid solutions are discussed.

1. Introduction

There is increasing interest in tunable and very short-pulse solid-state lasers during the last years due to their promising applications in modern science and technology. This stimulated the studies on single crystal materials with broadband emission in the near-infrared region, as tungstates [1–4], molybdates [5,6], borates [7,8], garnets [9,10], forsterite [11], germanates [12], alexandrite [13], galates [14] and silicates [15,16]. Cr-doped $NaAl(WO_4)_2$ is a potential laser-active medium because of its high absorption, efficient pumping with visible-range semiconductor diode lasers and broad laser emission [2]. The absorption cross-section of $NaAl(WO_4)_2$:Cr^{3+} attains values of 32×10^{-20} cm^2 for the $^4A_2 \rightarrow {}^4T_1$ transition and 17×10^{-20} cm^2 for the $^4A_2 \rightarrow {}^4T_2$ transition, respectively. For the sake of comparison, the values of the absorption cross-section of the Cr^{3+}-doped gadolinium scandium gallium garnet, GSGG:Cr^{3+}, are 5.1×10^{-20} and 3.3×10^{-20} cm^2 [17], and for alexandrite, 10×10^{-20} and 20×10^{-20} cm^2 [18], respectively. In addition, according to the spectral data of $NaAl(WO_4)_2$:Cr^{3+}, this new material shows a strong optical absorption in the 660–680 nm range where efficient pumping with laser diodes is possible [19].

However, the production of single crystals from this tungstate as laser active media is related to a number of problems, mainly due to anisotropy and low growth velocity [3]. An effective approach to circumvent crystal growth problems is to produce transparent ceramics to replace single crystals. Moreover, transparent ceramics are low-cost products of high chemical homogeneity and isotropy [20,21]. The technology of optical ceramics production includes three main stages:

1. synthesis of nanopowders.
2. preparation of high-density compacts.
3. sintering of the compacts to obtain non-porous ceramics.

The first step of $NaAl(WO_4)_2$ ceramic production is to obtain nanosized powder. Nanosized powder of non-doped $NaAl(WO_4)_2$ was successfully synthesized by us by a co-precipitation method [22]. In this way powders with the required dimensions, particle size distribution and particle shape were obtained. These characteristics are important for the next step of ceramic preparation.

The next step was the synthesis of Cr-doped $NaAl(WO_4)_2$. To this purpose it was important to find out the maximum amount of chromium, which can be accommodated in $NaAl(WO_4)_2$ without altering the structure.

$NaCr(WO_4)_2$ is an inorganic pigment with potential application in paints, ceramics, plastics and glasses [23,24]. The thermal and optical properties of this pigment may be modified by deep substitution of Cr by another element, e.g., Al.

The aim of the present work was to study the phase equilibria in the system $NaAl(WO_4)_2$–$NaCr(WO_4)_2$, with a view to determining the concentration crystallization regions of the phases and the influence of the concentrations of chromium and aluminium, respectively, on their basic thermal and structural characteristics. On the basis of the obtained data, Cr-doped $NaAl(WO_4)_2$ nanosized powders were synthesized for the first time with chromium concentration up to the highest admissible level.

* Corresponding author. Tel.: +359 2979 2786; fax: +359 2870 5024.
E-mail address: ikosseva@svr.igic.bas.bg (I. Koseva).

0025-5408/$ – see front matter © 2012 Elsevier Ltd. All rights reserved.
http://dx.doi.org/10.1016/j.materresbull.2012.06.061

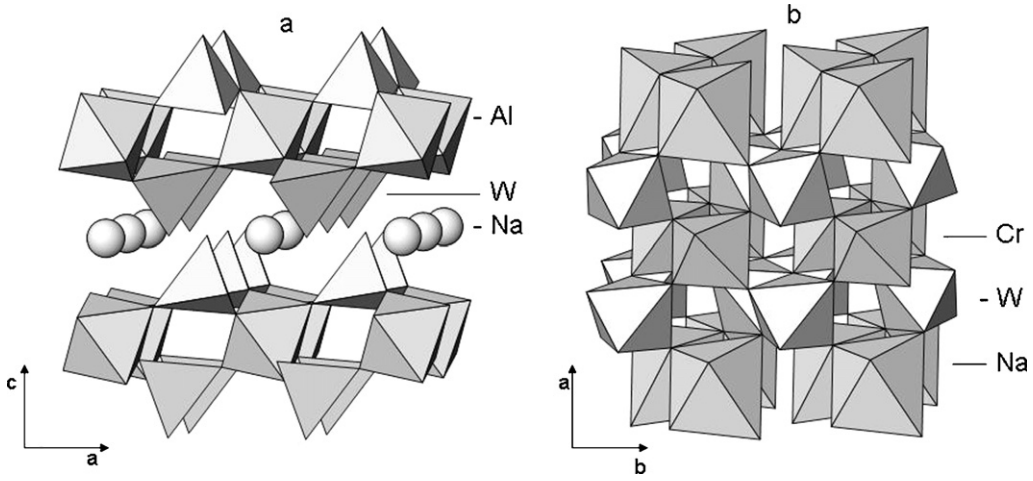

Fig. 1. The crystal structure of $NaAl(WO_4)_2$ along [0 1 0] direction (a) and the crystal structure of $NaCr(WO_4)_2$ along [0 0 1] direction (b).

2. Experiment and characterization techniques

$NaAl(WO_4)_2$ was synthesized by the co-precipitation method, described in our previous paper [22]. Aqueous solutions of $Na_2WO_4{\cdot}2H_2O$ and $Al(NO_3)_3{\cdot}9H_2O$ were mixed in a 3:1 molar ratio under intensive stirring. The obtained precipitate was filtered and dried at 80 °C. The dry product was thermally treated at 600, 650 or 700 °C for 1, 2 or 5 h. After multiple washing of the product, the final result was a pure single phase of $NaAl(WO_4)_2$. The described procedure was used for obtaining $NaAl_{1-x}Cr_x(WO_4)_2$ solid solutions. To this purpose the required molar parts of $Al(NO_3)_3{\cdot}9H_2O$ were substituted by relevant molar parts of $Cr(NO_3)_3{\cdot}9H_2O$. The percent ratio between the two nitrates was varied from 100:0 (pure $NaAl(WO_4)_2$) to 0:100 (pure $NaCr(WO_4)_2$).

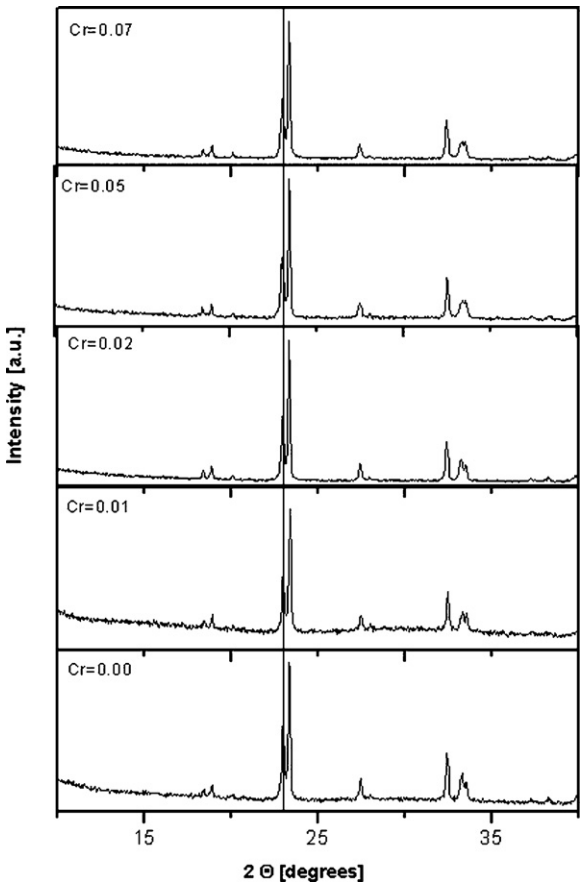

Fig. 2. X-ray powder diffractograms of products of Cr-doped $NaAl(WO_4)_2$, treated at 650 °C for 2 h, where the chromium concentration vary from 0 to 7 at% in the place of aluminium.

Powder X-ray diffraction patterns were recorded at room temperature on the Bruker D8 Advance diffractometer using CuKα radiation and LynxEye PSD detector within the range 10–80° 2θ. The X-ray pattern of a finely ground sample of $NaAl(WO_4)_2$ single crystal, obtained by the flux method in our previous work [3], was used as a reference in these analyses. The mean crystallite size and unit cell parameters were calculated from the integral breadth of all peaks (Pawley fit) using the TOPAS 3 program [25].

DTA/TG analysis of some of the synthesized products was performed on the LABSYSTM EVO DTA/TG device of SETARAM, France at a heating rate of 10 °C/min in Ar flow at a flow rate of 20 ml/min.

Additional information about the size and shape of the particles of some of the samples was obtained by TEM analyses using the TEM JEOL 2100 instrument at 200 kV. To this purpose specimens were prepared by grinding the samples in an agate mortar and dispersing them in methanol by ultrasonic treatment for 6 min. A droplet of the suspension was dispersed on holey carbon films on Cu grids.

The SEM micrographs were obtained on a Philips SEM 515 device at an accelerating voltage of 20 kV. The powders were covered with a gold layer of 10–15 nm thickness.

3. Results and discussion

It is known that $NaAl(WO_4)_2$ crystallizes in monoclinic structure, space group C2/c [26,27]. This structure can be represented as chains of edge-linked aluminium and sodium octahedra forming a three-dimensional network of WO_4 tetrahedra with shared oxygen atoms (Fig. 1a).

Table 1
Calculated cell parameters values a, b, c and β of $NaAl_{1-x}Cr_x(WO_4)_2$, space group C2/c, depending on the Cr-concentration.

Cr [at%]	a [Å]	b [Å]	c [Å]	β [°]
0.0	9.622	5.382	12.977	90.11
1.0	9.630	5.378	12.993	90.12
2.0	9.631	5.382	12.990	90.19
5.0	9.644	5.376	13.017	90.19
7.0	9.652	5.385	13.027	90.20